

# **Contrasted projection of the ENSO-driven CO<sub>2</sub> flux variability in the Equatorial Pacific under high warming scenario: supplementary**

Pradeebane Vaittinada Ayar<sup>1</sup>, Jerry Tjiputra<sup>1</sup>, Laurent Bopp<sup>2</sup>, Jim R. Christian<sup>3</sup>, Tatiana Ilyina<sup>4</sup>, John P. Krasting<sup>5</sup>, Roland Séférian<sup>6</sup>, Hiroyuki Tsujino<sup>7</sup>, Michio Watanabe<sup>8</sup>, and Andrew Yool<sup>9</sup>

<sup>1</sup>NORCE Norwegian Research Centre AS, Bjerknes Centre for Climate Research, Bergen, Norway

<sup>2</sup>LMD-IPSL, Ecole Normale Supérieure / Université PSL, CNRS, Ecole Polytechnique, Sorbonne Université, Paris, PSL University, Paris, France

<sup>3</sup>Canadian Centre for Climate Modelling and Analysis, Victoria, BC, CA

<sup>4</sup>Max Planck Institute for Meteorology, Hamburg, Germany

<sup>5</sup>NOAA/Geophysical Fluid Dynamics Laboratory, Princeton, New Jersey 08540, USA

<sup>6</sup>CNRM, Université de Toulouse, Météo-France, CNRS, Toulouse, France

<sup>7</sup>JMA Meteorological Research Institute, Tsukuba, Ibaraki, Japan

<sup>8</sup>Research Institute for Global Change, Japan Agency for Marine-Earth Science and Technology (JAMSTEC), 3173-25, Showa-machi, Kanazawa-ku, Yokohama, Kanagawa, 236-0001, Japan

<sup>9</sup>National Oceanography Centre, Southampton, UK

**Correspondence:** Pradeebane Vaittinada Ayar, (paya@norceresearch.no;pradeebane@laposte.net)

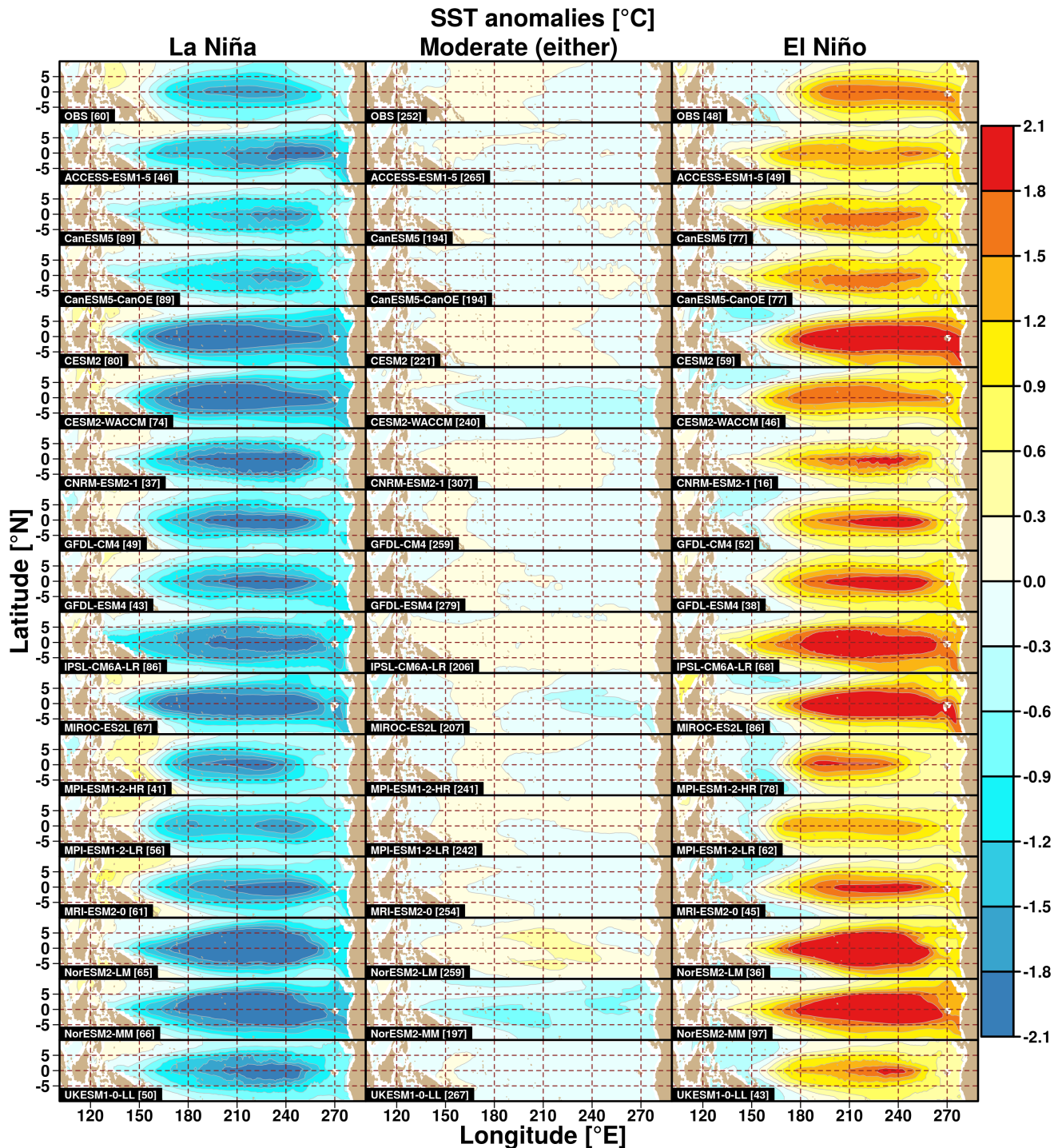


**Figure S 1.** CMIP6 ensemble SST (in °C) average anomalies over the 1985-2014 contemporary period for the La Niña, El Niño and the moderate regimes.

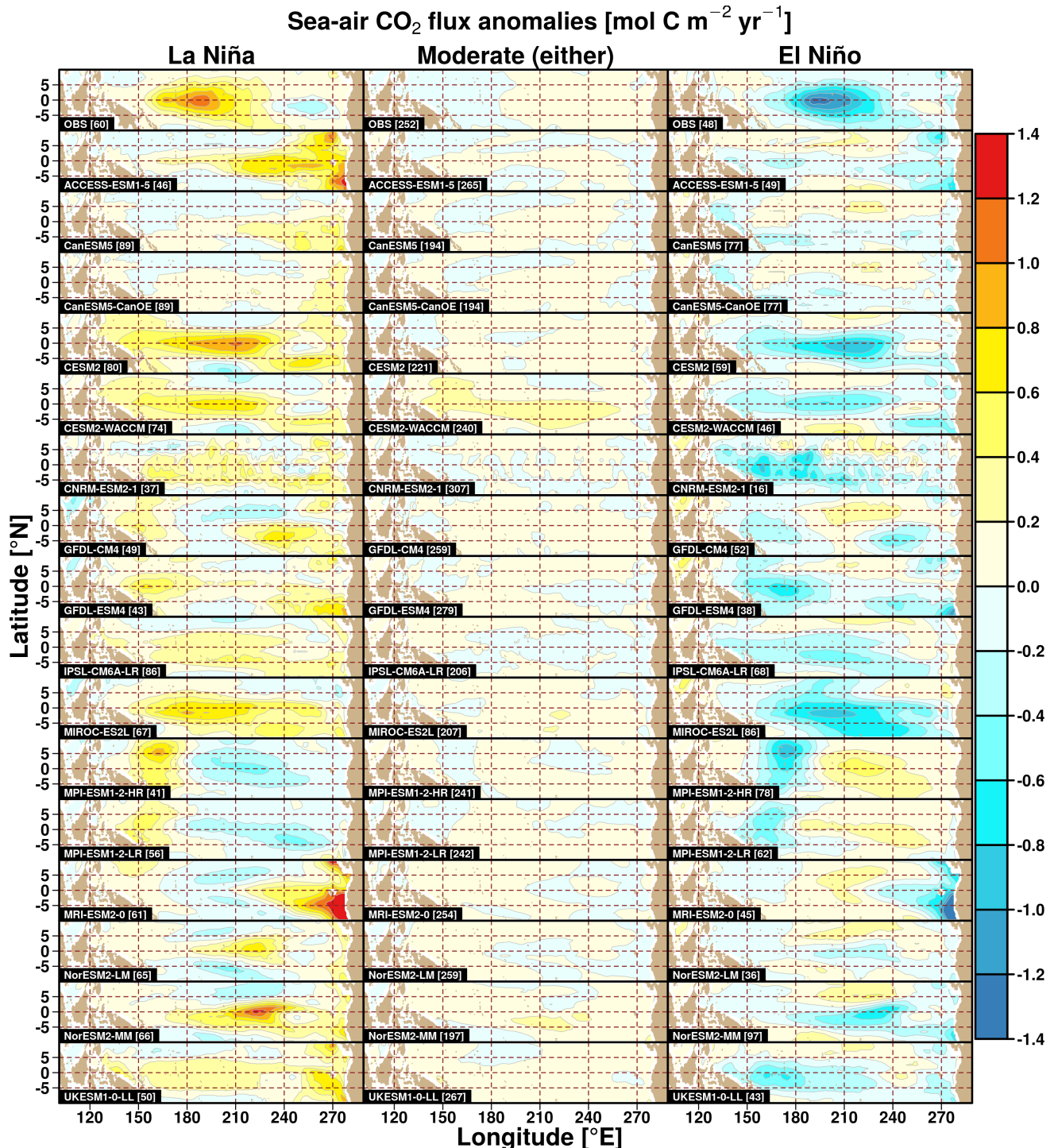


**Figure S 2.** CMIP6 ensemble sea-air CO<sub>2</sub> fluxes (in mol C m<sup>-2</sup> yr<sup>-1</sup>) average anomalies over the 1985-2014 contemporary period for the La Niña, El Niño and the moderate regimes.

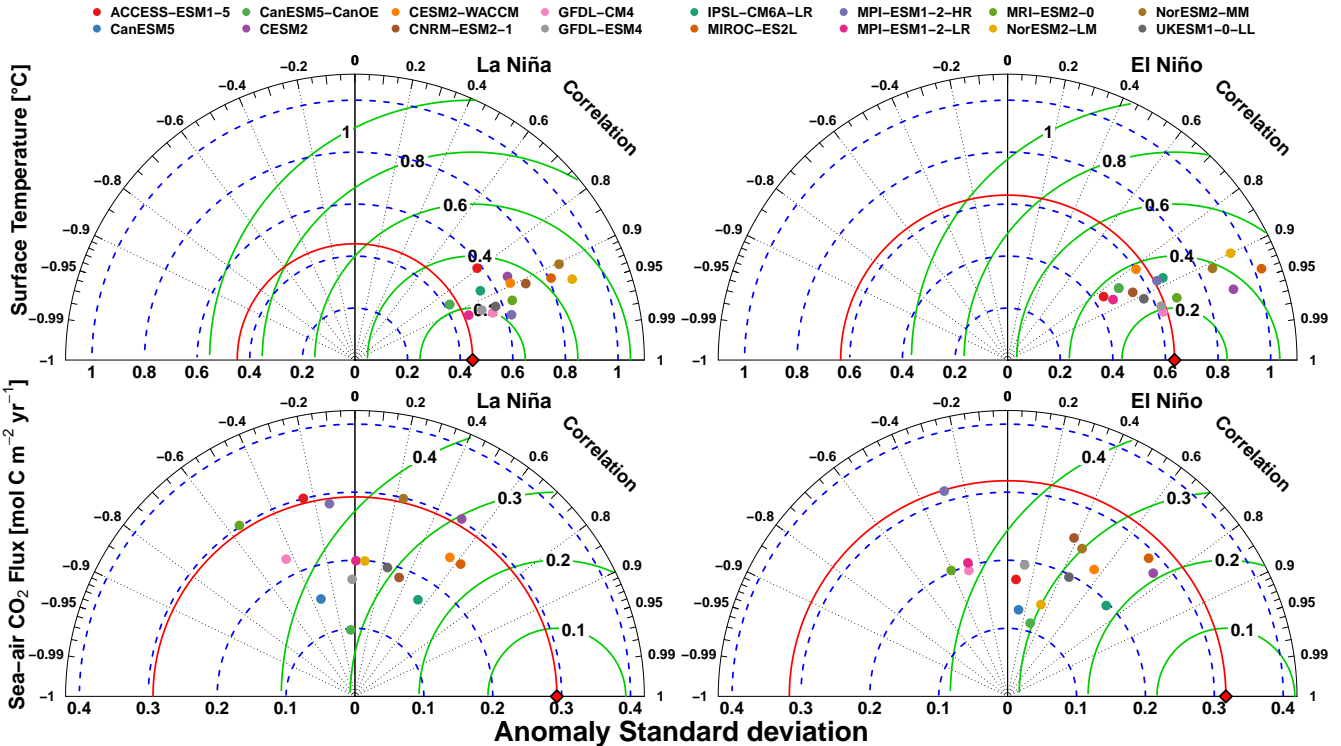


**Figure S 3.** Taylor diagramme of CMIP6 ensemble SST (in  $^{\circ}\text{C}$ , top) and sea-air CO<sub>2</sub> fluxes (in  $\text{mol C m}^{-2} \text{yr}^{-1}$ , bottom) average anomalies over the 1985-2014 contemporary period for the La Niña and El Niño regimes. Reference values (observed mean values in our case) correspond to the red diamond on the abscissa. Radial distances from the origin are proportional to the standard deviation (blue dashed lines) while azimuthal positions give the correlation coefficient between the simulated and observed values. Finally the green circular lines correspond to the 'centred'-RMSE.

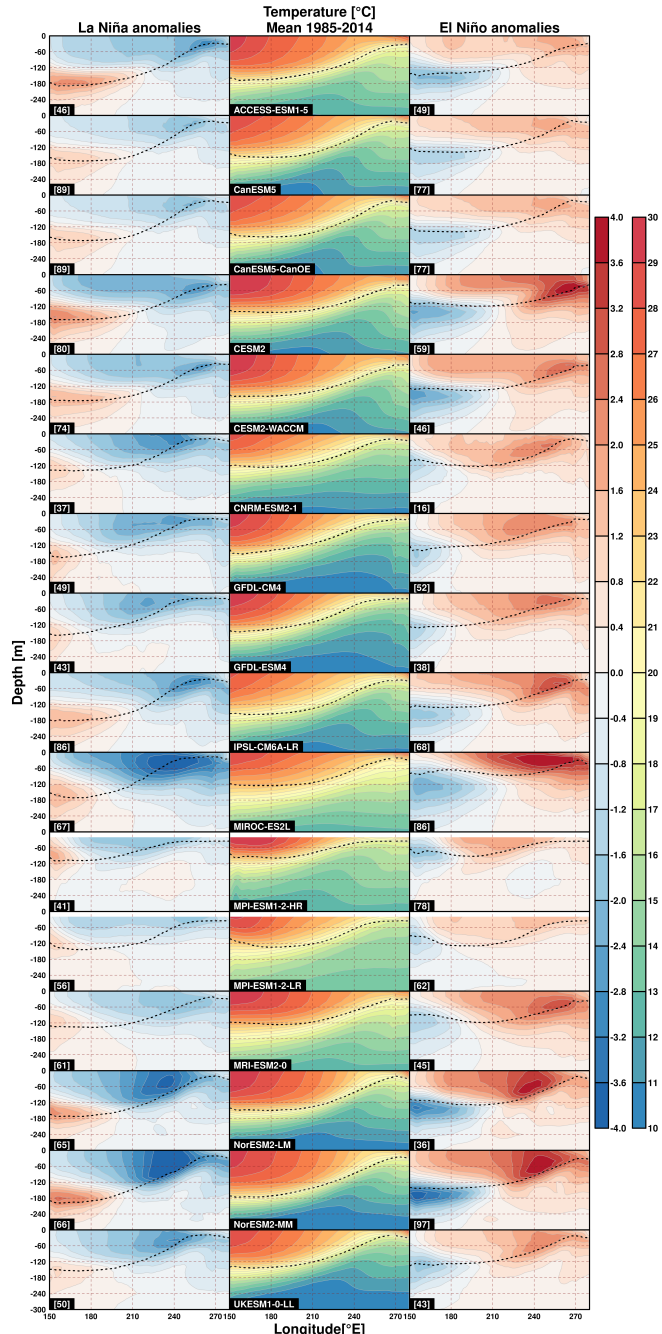


**Figure S 4.** CMIP6 ensemble vertical section of temperatures (in  $^{\circ}\text{C}$ ) zonal (between  $\pm 2^{\circ}\text{N}$ ) average over the 1985-2014 contemporary period (*middle*). Average anomalies (differences) relative to contemporary mean are given for La Niña (*left*) and El Niño (*right*) regimes. Dotted lines indicate the average thermocline depth. In square brackets, the number months in each regime for each CMIP6 models.

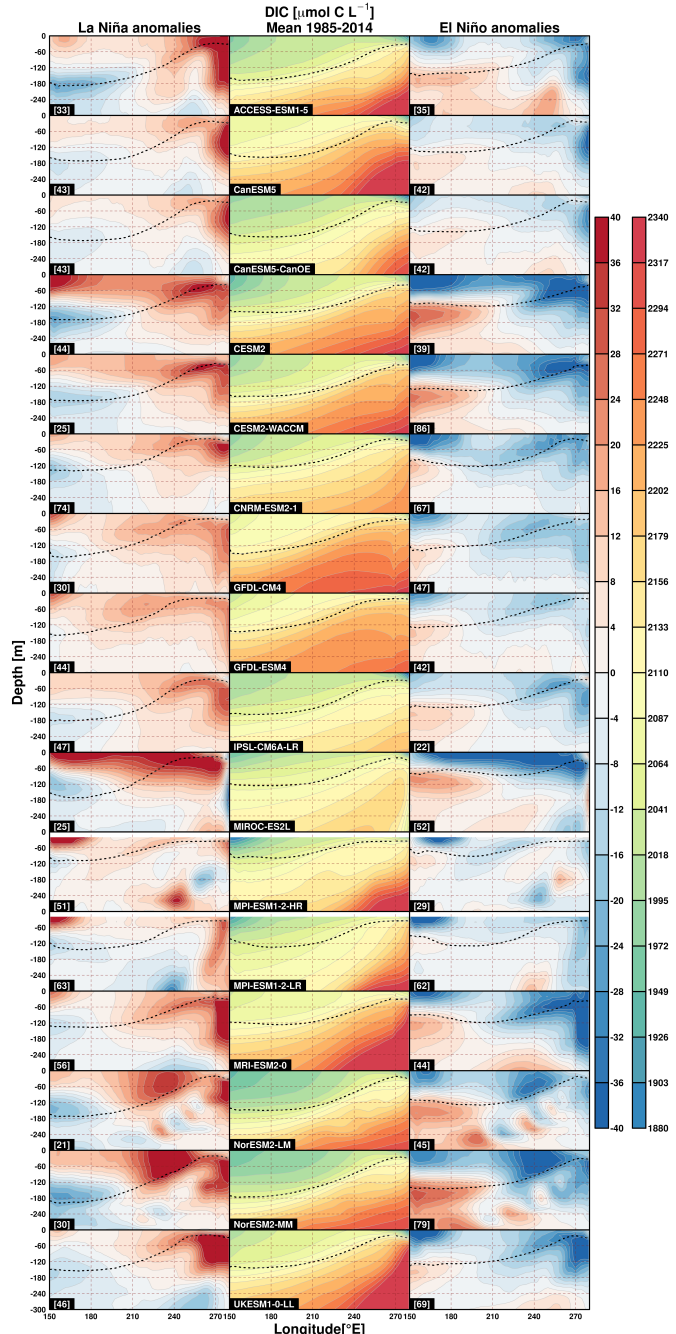


**Figure S 5.** CMIP6 ensemble vertical section of DIC (in  $\mu\text{mol L}^{-1}$ ) zonal (between  $\pm 2^\circ\text{N}$ ) average over the 1985-2014 contemporary period (middle). Average anomalies (differences) relative to contemporary mean are given for La Niña (left) and El Niño (right) regimes. Dotted lines indicate the average thermocline depth. In square brackets, the number months in each regime for each CMIP6 models.

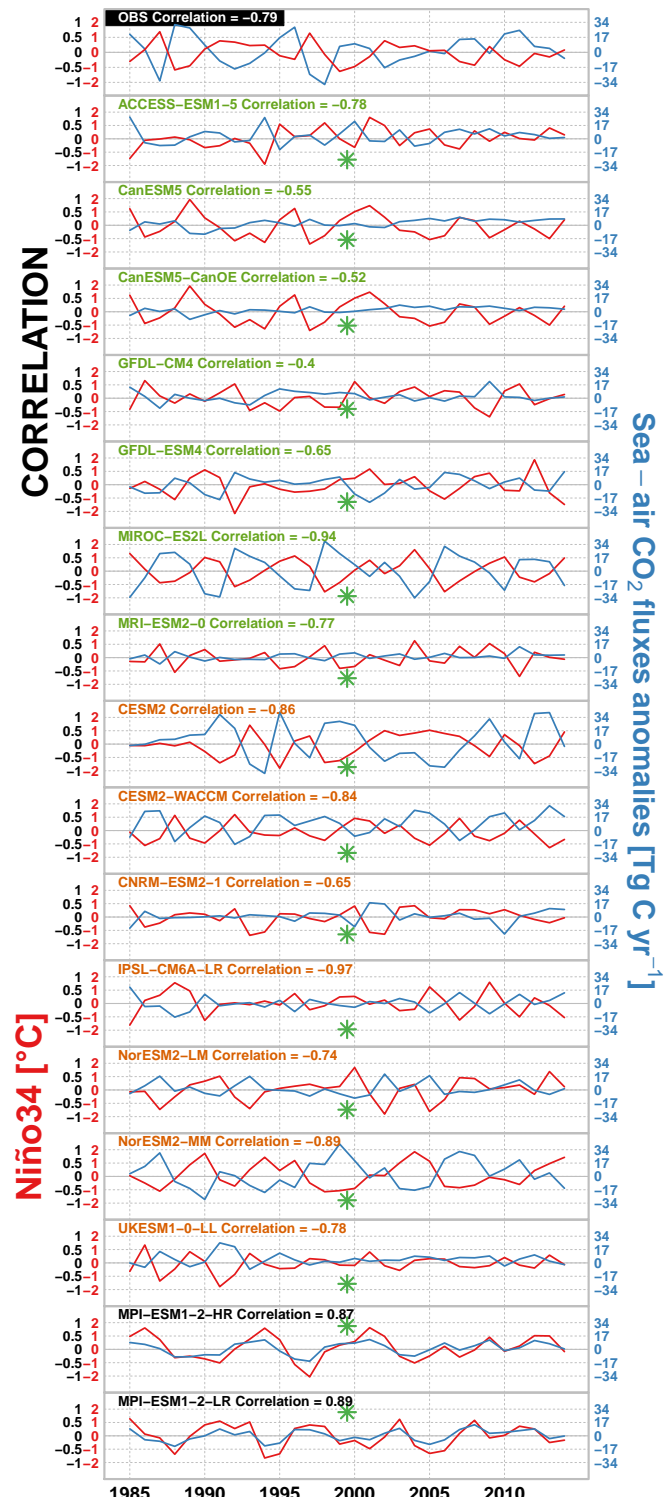


**Figure S 6.** Same as Figure 3 but for the 1985–2014 contemporary period.

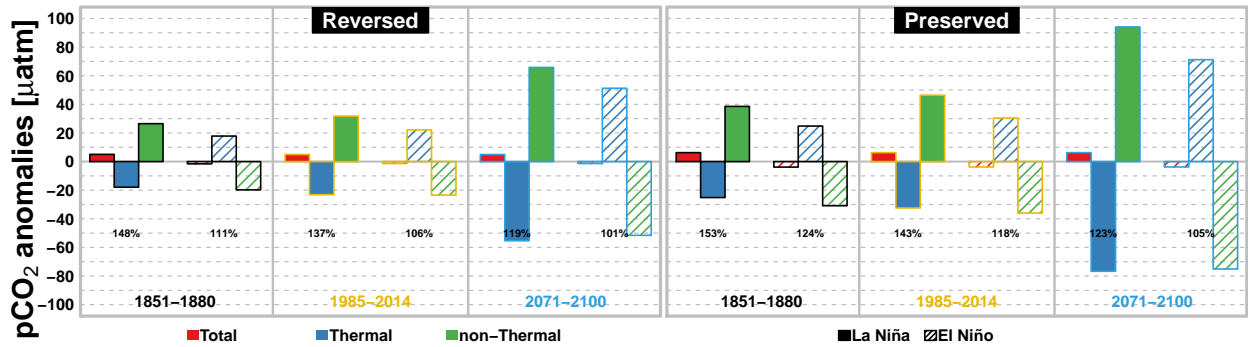


**Figure S 7.** El Niño and La Niña average of total (in red), thermal (in blue) and non-thermal (in green)  $p\text{CO}_2$  mean anomalies (in  $\mu\text{atm}$ ) for the reversed (left) and preserved (right) ESMs over the early historical (1851–1880) in EP domain. The same components are estimated by scaling the background  $p\text{CO}_2$  scaled to contemporary (1985–2014) and future (2071–2100) periods. The absolute ratio between the non-thermal and thermal component is given (in %) for each periods, groups and ENSO phases.

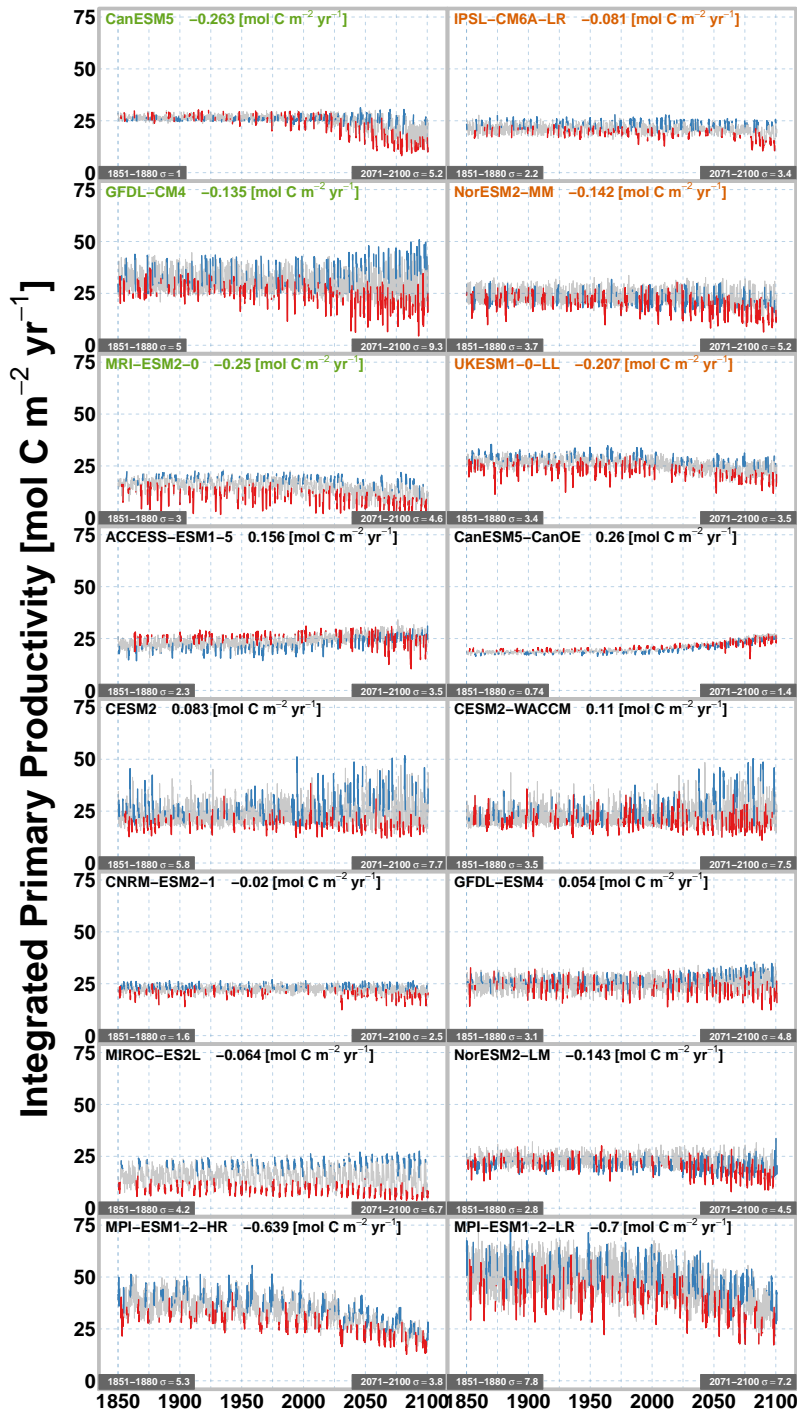


**Figure S 8.** Time-series of intPP (in  $\text{mol C m}^{-2} \text{yr}^{-1}$ ) from 1850 to 2100. The blue and red colours indicates the occurrence of the La Niña and El Niño regimes. The decadal trend is given for each model. Models names are given in green for the models with shifting correlation sign, in orange for those maintaining the negative correlation and black the others. The intPP standard deviation ( $\sigma$ ) over the early historical (1851–1880) and future (2071–2100) periods are given for each model.

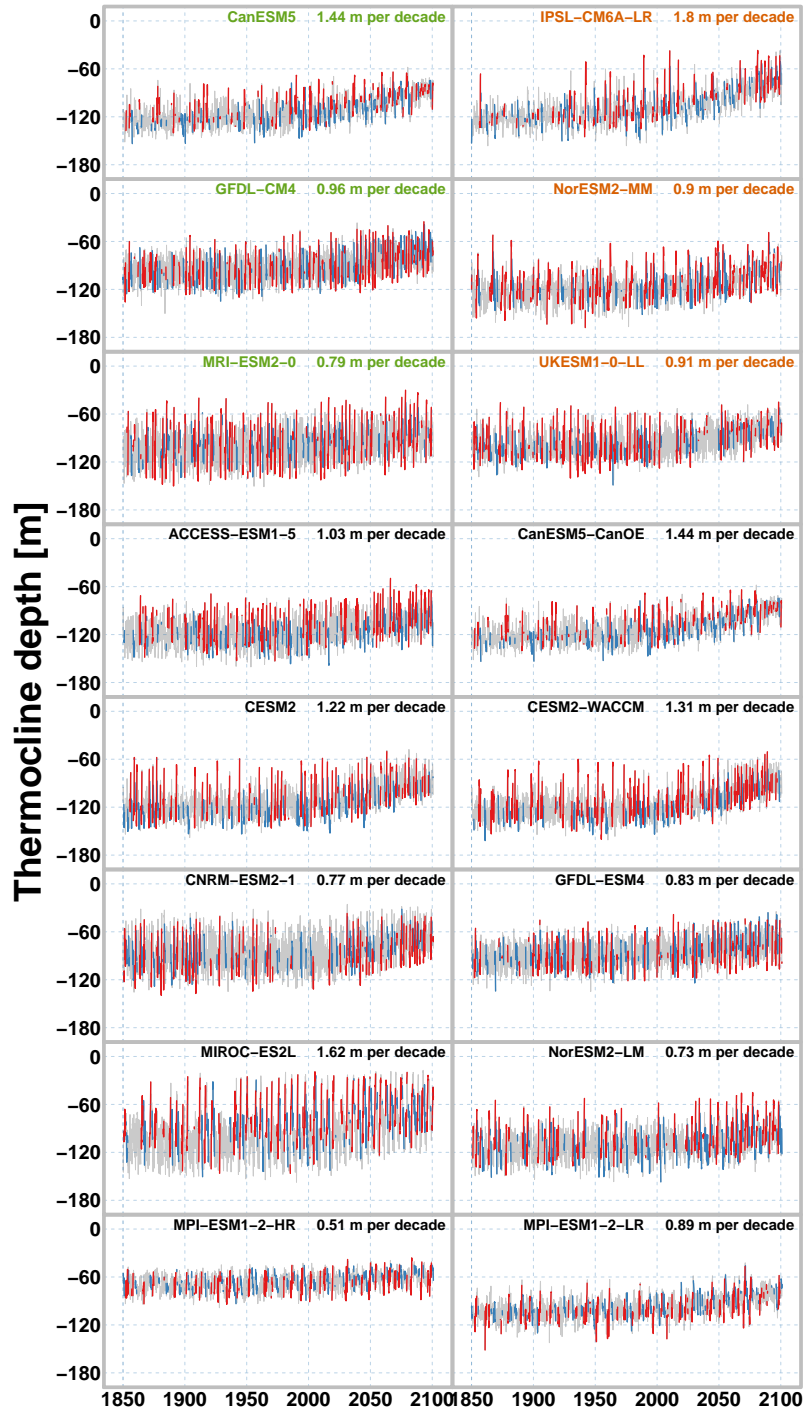


**Figure S 9.** Time-series of thermocline depth (in m) from 1985 to 2100. The blue and red colours indicates the occurrence of the La Niña and El Niño regimes. The decadal trend is given for each model. Models names are given in green for the models with shifting correlation sign, in orange for those maintaining the negative correlation and black the others.

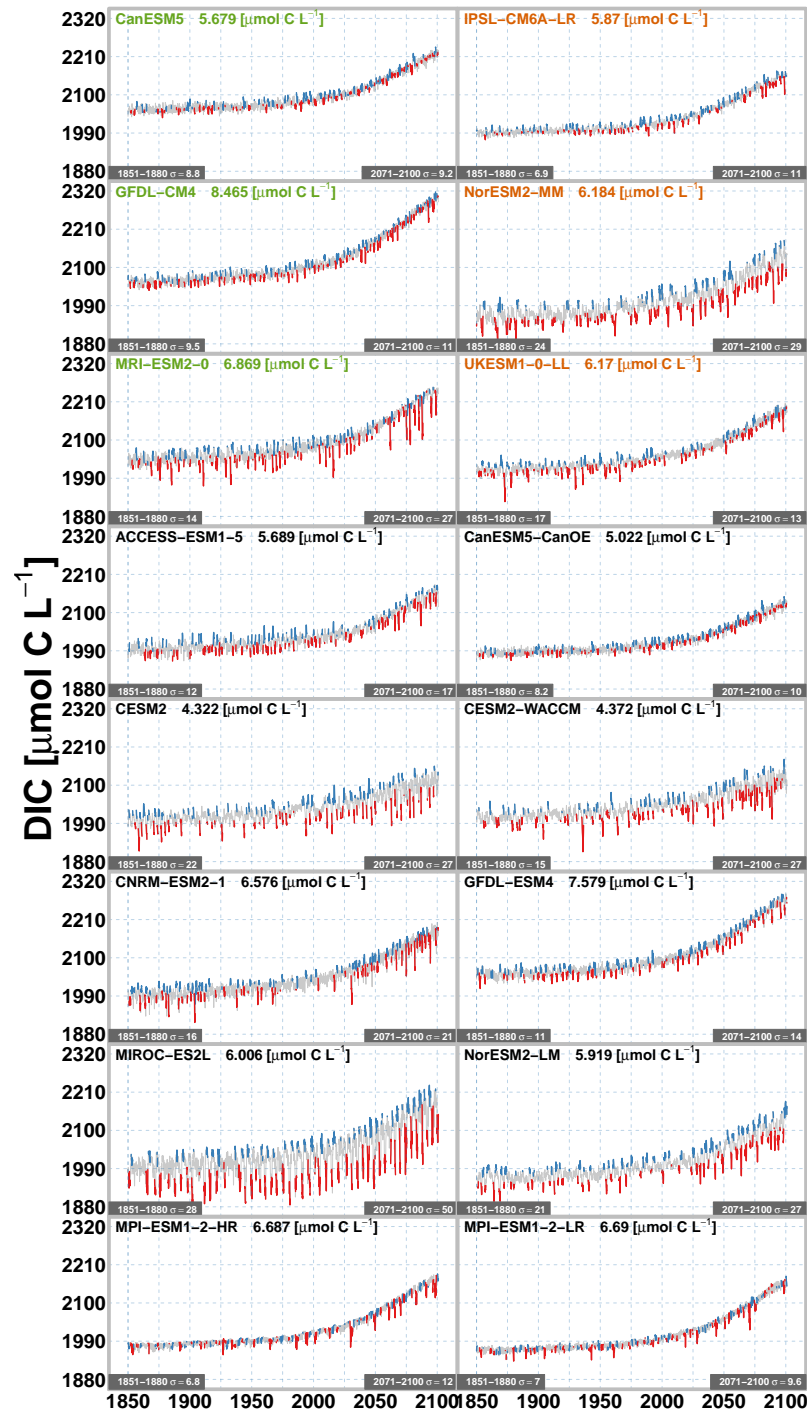


**Figure S 10.** Time-series of average surface DIC (left in  $\mu\text{mol C L}^{-1}$ ) from 1985 to 2100. The blue and red colours indicates the occurrence of the La Niña and El Niño regimes. The decadal trend is given for each model. Models names are given in green for the models with shifting correlation sign, in orange for those maintaining the negative correlation and black the others. The DIC standard deviation ( $\sigma$ ) over the early historical (1851–1880) and future (2071–2100) periods are given for each model.